SPECTRAL DISTRIBUTIONS OF DIFFUSE AND GLOBAL IRRADIANCE FOR CLEAR AND CLOUDY PERIODS

Gina Blackburn
Department of Physics
1274-University of Oregon
Eugene, Or 97403-1274
e-mail: blackbur@uoregon.edu

Frank Vignola
Department of Physics
1274-University of Oregon
Eugene, Or 97403-1274
e-mail: fev@uoregon.edu

ABSTRACT

An LI-1800 Portable Spectroradiometer is used to measure solar spectral irradiance for solar zenith angles of 53.5º to 86.3º during the months of January, February, and March. Data is collected showing global horizontal and diffuse irradiance for clear and cloudy days, and then used in the analysis of an LI-200 pyranometer to predict responsivities under different conditions. It is shown that the global horizontal irradiance has a similar spectral distribution for both clear and overcast periods and that the diffuse horizontal component is significantly affected by clear and cloudy periods.

1. INTRODUCTION

In the field of solar energy, the characterization of spectral irradiance is an important issue. As the field of photovoltaics expands and more and more investors seek to replace "conventional" energy systems with solar power units, the researchers' ability to predict the future cost and efficiency of photovoltaic (PV) cells after installation becomes ever more vital. A concrete understanding of the composition of spectral irradiance and how it will be effected by its surroundings is therefore a topic of great interest and can be used to develop broader and more accurate simulation techniques. Spectral irradiance data is also important for the development of accurate instrument calibration methods. As discussed in Lopez and Chenlo (1), as well as Vignola (2), many materials, including PV cells, exhibit spectrally dependent responses and must therefore be well calibrated in order to give good quality measurements.

Among the factors affecting the magnitude and distribution of spectral irradiance, the sun's angle with respect to the measurement location, pollution, and weather conditions play a significant role. Research pertaining to the effect of seasonal variation on solar spectral irradiance can be found in Lopez and Chenlo (1). Programs simulating clear period spectral distributions have seen considerable success and continue to be developed and improved, see for example Gueymard's SMARTS program (3). Simulating spectral irradiance for cloudy or diffuse conditions, however, has proved to be a more difficult task to accomplish.

In this paper, data is presented from measurements of global horizontal irradiance (GHI), and diffuse horizontal irradiance (DHI) for clear and cloudy periods, taken with an LI-1800 Portable Spectroradiometer (the term "cloudy period GHI" will be used throughout this paper, although for cloudy conditions, as the clouds block the direct beam component, GHI and DHI are really the same thing). Three typical measurements are compared, and similarities in the distributions for clear and cloudy period GHI and clear period DHI are examined and discussed. The response curve for a typical LI-200 pyranometer (an instrument often used for measuring spectral irradiance, and one with a spectrally- dependent response), is then used together with the measurements from the LI-1800 to predict responsivities for the LI-200 for different solar zenith angles and weather conditions. From this data, significant similarities in GHI for clear and cloudy periods can be seen, and the differences observed in the clear period DHI are discussed.

2. SETUP

Measurements were taken with an LI-1800 Portable Spectroradiometer, manufactured by LI-COR Biosciences in Lincoln, Nebraska. The LI-1800 uses a silicon photodiode operating in the photovoltaic mode, meaning that it has its own spectral response curve. This is present in a calibration file that is used to rectify collected data

after measurements are taken. While the LI-1800 is no longer manufactured, service will be provided until the end of 2012 and technical support will continue after that (4). The experimental setup is pictured in Fig. 1. Measurements were taken at the University of Oregon Solar Radiation Monitoring Lab in Eugene, Oregon. A leveling block and bubble level were used to assure that the detector was horizontal, and a water cooling system was used to keep the detector at a constant temperature of 18 ºC. For clear days, data was collected with the addition of a 2-inch diameter sunshade positioned approximately 19.74 inches from the cosine receptor at an angle of 5.7º.

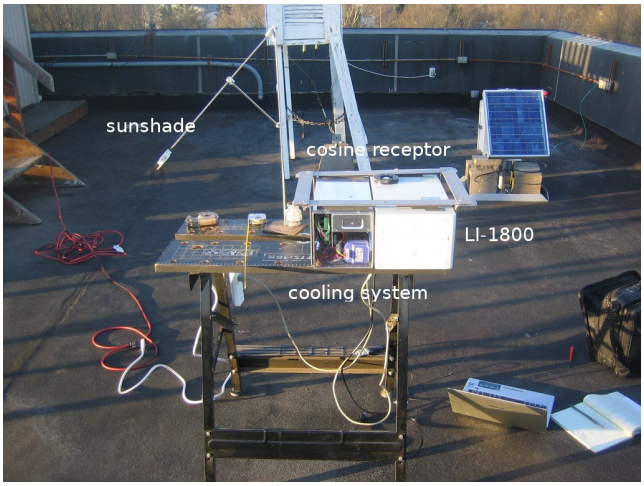

Fig. 1: Experimental Setup showing the LI-1800 Spectroradiometer, sunshade, and cooling system. The opening to the detector (called the cosine receptor) is also visible

When using a sunshade it is customary to use a blackened disk so that light will not be reflected back into the detector from the disk face. For this project, we used an unblackened metal disk, which could have resulted in some reflection. Furthermore, the design of the cosine receptor on the LI-1800 is such that the receptor dome sits in a black collar, the edges of which are slightly raised with respect to the receptor dome. This collar is a design feature which gives the detector a better cosine response, although for angles greater than about 72º, the cosine receptor begins to shade itself. Some measurements were taken with as much as 45% of the cosine receptor self-shaded. It is possible that this causes the dip in the clear period GHI responsivity in Fig. 6 for angles greater than 82º. A third issue is one of weather conditions and geographic location. January through March is a disproportionately rainy period in Eugene, and it was not always possible to measure GHI and DHI for completely clear days (that is, completely absent of haze or light cloud trails). As a result, some measurements may exhibit effects from interactions with some light haze. Particularly suspect are values in Fig. 6 for clear day GHI and clear day DHI which appear to rise significantly above the others at around 80º.

3. RESULTS

Global and diffuse horizontal irradiance was measured between January 31, 2012 and March 8, 2012 for a range of solar zenith angles from 53.5º to 86.3º under clear and cloudy conditions. A comparison of three such measurements can be seen below in Fig. 2 and 3.

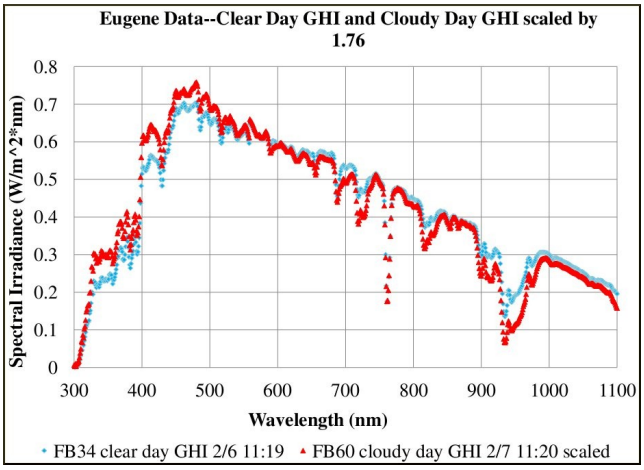

Fig. 2: Clear period GHI (red) taken on 2/6/2012 at 11:19, cloudy period GHI scaled by 1.76 (purple) taken 2/7/2012 at 11:20

Fig. 2 shows a typical clear period GHI measurement(red), and and a typical cloudy period GHI measurement (purple). The cloudy period GHI has been scaled by a factor of 1.76 (area normalized to the plot of clear period GHI) to facilitate comparison. It is seen that the two distributions closely resemble one another.

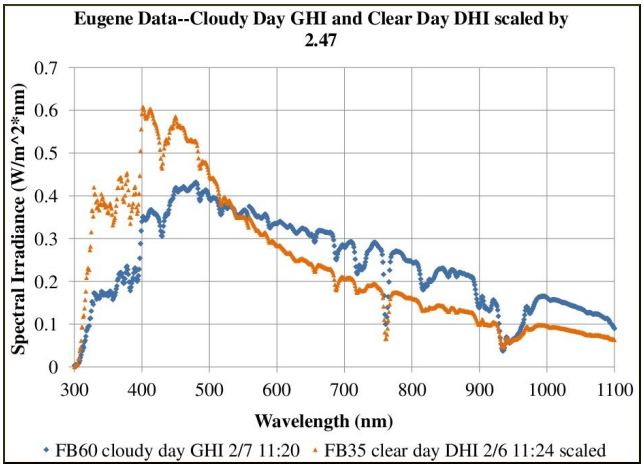

Fig. 3: Cloudy period GHI (blue) taken 2/7/2012 at 11:20, clear period DHI scaled by 2.47 (orange) taken 2/6/2012 at 11:24

Fig. 3 shows a typical measurement of cloudy period GHI (blue), and a typical measurement of clear period DHI (orange). The clear period DHI has been scaled by a factor of 2.47 (area normalized to the plot of cloudy period GHI) to facilitate comparison. Unlike those in Fig. 2, where the two distributions were seen to be fairly similar, at least in form, the measurements in Fig. 3 have significantly different shapes to their distributions, especially notable in the shorter wavelengths.

4. ANALYSIS

The LI-200 pyranometer, shown in Fig. 4, like the LI-1800, measures global horizontal irradiance using a silicon photodiode.

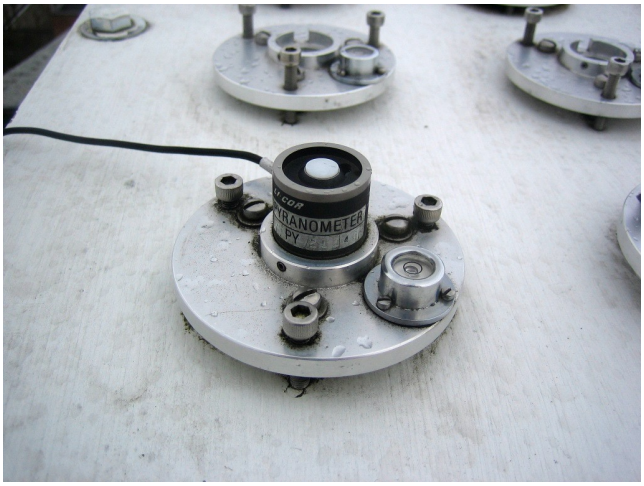

Fig. 4: LI-200 Pyranometer

A response curve pictured in Fig. 5 has been determined from plots provided by the LI-COR Terrestrial Radiation Sensors Instruction Manual (5). It is visible in Fig. 5 that the LI-200's response has a range of 400 nm to 1100 nm and is wavelength-dependent, with a peak response at 950 nm. The response curve is approximately linear between 450 and 950 nm, and it can be seen from the figure that the LI-200 has a higher response for longer wavelengths.

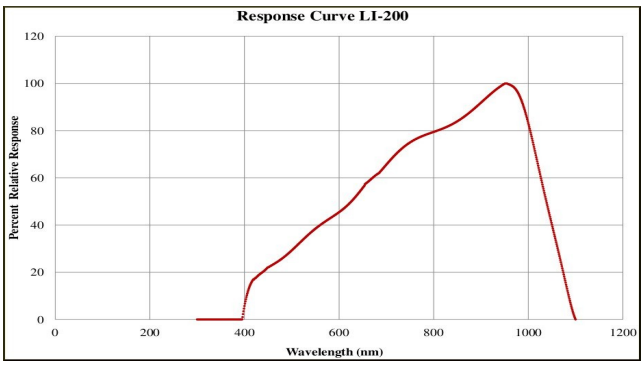

Fig. 5: Response curve of a typical LI-200 pyranometer

Values from the LI-200 response curve and the data from the LI-1800 were used to calculate responsivities according to Equation 1.

$$R = \frac{\sum_{\lambda=300}^{1100} R(\lambda) I(\lambda)}{\sum_{\lambda=300}^{1100} I(\lambda)} \qquad (1)$$

Fig. 6 shows these responsivities, calculated for measurements of global and diffuse horizontal irradiance made between January 31 and March 8, during clear and cloudy periods. It is seen from the figure that the responsivities for clear and cloudy period GHI are very similar while the responsivities for clear day DHI are much lower, with a slight increase at greater solar zenith angles.

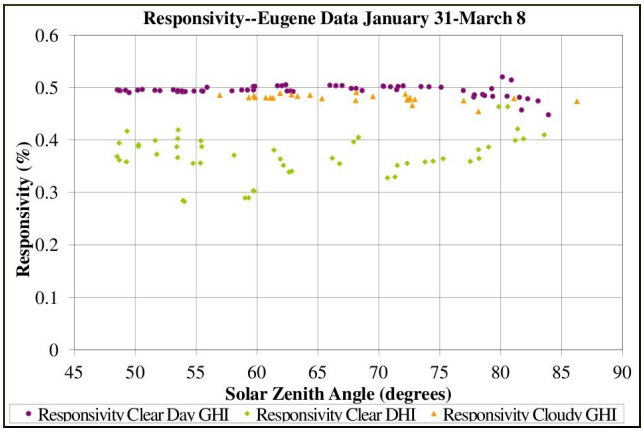

Fig. 6 Responsivities for clear day GHI (purple circles), clear day DHI (green diamonds), cloudy day GHI (orange triangles)

5. DISCUSSION

As seen in Fig. 2 and 3, the GHI distributions for clear and cloudy periods exhibit many similarities while a comparison of clear period DHI and cloudy period GHI suggests that DHI distributions differ significantly. The similarities in clear and cloudy period GHI distributions can be explained by the relatively large size of the cloud particles, which causes the clouds to act as “neutral density filters”, scattering all wavelengths equally. Although not visible for the scaled version of the cloudy period GHI presented in Fig. 2, less irradiance is measured under cloudy conditions, which is due to the absence of the direct normal component and the reflection of light from the clouds back into the atmosphere (2).

The unique shape of the DHI distribution in Fig. 3 can be explained by the effect of Rayleigh scattering in the atmosphere, which is inversely proportional to the fourth

power of the wavelength, with the result that shorter wavelengths will be more prevalent in scattered light. To an observer for whom the sun is close to the horizon (for example in the evening), a longer path length through the atmosphere in combination with Rayleigh scattering will cause the diffuse component to appear more reddish orange (6).

In Fig. 5, it is seen that the responsivities for clear and cloudy period GHI are fairly consistent with each other, with cloudy period GHI appearing to be slightly lower. The responsivities for clear period DHI were seen to be significantly lower with a slight increase towards the larger solar angles. As can be seen from the response curve in Fig. 6, the LI-200 responds best for longer wavelengths. As already discussed, Rayleigh scattering causes shorter wavelengths to dominate the diffuse component during clear periods, which can explain why, for smaller solar zenith angles, the clear period DHI responsivity of the LI-200 is much lower than that for clear and cloudy GHI. As the solar zenith angle increases, however, the scattered light will experience a shift in wavelength as it passes through a larger volume of atmosphere, causing longer wavelengths to dominate. This may cause the increase seen in Fig. 6 for angles greater than 80º.

It would be useful to expand on this research in the future by collecting data for a wider range of solar zenith angles.

6. CONCLUSION

In this paper, three measurements from the LI-1800 were plotted (clear period GHI, cloudy period GHI, and clear period DHI), using scaled versions of certain measurements to facilitate comparison. Similarities in the cloudy period GHI and clear period GHI distributions were explained by the equal scattering of wavelengths from the comparatively large cloud particles present under overcast conditions, while the clear period DHI measurements exhibited a spectral dependence, explained by the higher proportion of Rayleigh-scattered short wavelengths present in diffuse light under clear conditions.

A response curve for the LI-200 pyranometer was determined from existing plots and, using this data along with Equation 1 and measurements made by the LI-1800, responsivities were calculated and presented in Fig. 6. The plotted data agrees with what is seen in Fig. 2 and 3.

The data suggests that the spectral irradiance distributions on clear and cloudy days will be similar to each other throughout the day for the global horizontal irradiance, but that the diffuse component will depend somewhat on the solar zenith angle. It is also shown that the responsivities of a typical LI-200 pyranometer should be similar for measurements of clear and cloudy period global horizontal irradiance, but that the responsivity of the diffuse horizontal component will vary with the distribution of incident wavelengths.

As discussed in previous papers (see 7 and 8), these results hold special significance for instruments which use photodiode detectors such as LI-200 pyranometers as well as certain models of Rotating Shadowband Pyranometers (RSPs). These devices calculate direct normal irradiance from measurements of global horizontal irradiance and diffuse horizontal irradiance. For RSPs using photodiode detectors (such as the LI-200), the diffuse component will depend heavily on the angle of the sun and the weather conditions, as has been shown in previous research (7 and 8), as well as in the results discussed in this paper. This can lead to an underestimation of the diffuse irradiance and a subsequent overestimation of the direct beam component (8). These results are also important for PV materials, which have a response curve greatly resembling that of an LI-200, implying that they may behave similarly for the conditions discussed in this paper.

7. ACKNOWLEDGEMENTS

The sponsors of the University of Oregon Solar Radiation Monitoring Laboratory should be acknowledged for support of our efforts to build a high quality solar radiation database in the Pacific Northwest. The sponsors are, the Bonneville Power Administration, Energy Trust of Oregon, and Oregon Best.

8. REFERENCES

(1) Perez-Lopez, J.J., Fabero, F., Chenlo F. (2007). Experimental Solar Spectral Irradiance Until 2500 nm: Results and Influence on the PV Conversion of Different Materials. Prog. Photovolt: Res. Appl. 2007; 15:303-315. Published online November 21, 2006 in Wiley InterScience http://www.wiley.interscience.com}
(2) Vignola, F., Michalsky, J., Stoffel, T. (2013). Solar and Infrared Radiation Measurements. CRC Press, Taylor & Francis Group, June, 2012.
(3) Gueymard, C. (2007). Prediction and validation of cloudless shortwave solar spectra incident on horizontal, tilted, or tracking surfaces. Solar Energy, 82(2008), 260-271.
(4) LI-COR Bionsciences (1991). LI-1800 Portable Spectroradiometer Instruction Manual. Nebraska: LI-COR.
(5) LI-COR Biosciences (2005). LI-COR Terrestrial Radiation Sensors Instruction Manual. Nebraska: LI-COR.
(6) Giancoli, D. (2005). Physics: Principles with Applications. Prentice Hall: Pearson
(7) Vignola, Frank. Solar Cell Based Pyranometers:

Evaluation of the Diffuse Response, Proceedings of the 1999 Annual Conference, American Solar Energy Society, 260, June 1999.
(8) Vignola, F. (2006). Removing Systematic Errors from Rotating Shadowband Pyranometer Data. Proc. of the 35th ASES Annual Conference. Denver, CO.